REPORT No. 393

SPAN-LOAD DISTRIBUTION AS A FACTOR IN STABILITY IN ROLL

By MONTGOMERY KNIGHT and RICHARD W. NOYES

SUMMARY

This report gives the results of pressure-distribution tests made to study the effects on lateral stability of changing the span-load distribution on a rectangular monoplane wing model of fairly thick section. Three methods of changing the distribution were employed: variation in profile along the span to a thin symmetrical section at the tip, twist from +5° to −15° at the tip, and sweepback from +20° to −20°. The tests were conducted at the Langley Memorial Aeronautical Laboratory in the 5-foot closed-throat atmospheric wind tunnel.

The rolling moment due to roll at a rate of rotation equivalent to that resulting from the maximum rolling disturbances encountered in normal flight is used as the principal basis of comparison. Normal-force curves are given for the purpose of estimating the general effectiveness of each wing arrangement.

The investigation shows the following outstanding results:

1. Change in profile along the span from the N. A. C. A. 84 at the root to the N. A. C. A.–M2 at the tip considerably reduces lateral instability, but also reduces the general effectiveness of the wing.

2. Washout up to 11° progressively reduces maximum lateral instability.

3. Transition from sweepforward to sweepback gradually reduces the useful angle-of-attack range, but has no clearly defined effect on maximum lateral instability.

INTRODUCTION

The problem of reducing the unstable rolling tendency due to roll, characteristic of unyawed, stalled flight, has been attacked in various ways. The earliest methods consisted of attempts to improve lateral controllability by increasing the rolling moments produced by the ailerons. These methods enabled the pilot to correct for disturbances more effectively, but did not remove the source of the danger, the rolling tendency itself. Subsequent developments resulted in the use of such devices as the Handley Page automatic slot and the wing tip floating aileron, both of which have been shown not only to reduce the unstable rolling tendency due to roll but also to improve the controllability.

Another method for reducing lateral instability is the modification of the shape of the conventional wing. The nature of the modifications best suited to this purpose may be determined from a consideration of the factors controlling rolling moment due to roll. Primarily, this moment depends upon the distribution of load along the span when the wing is given an angular velocity in roll. This distribution is dependent upon the variation of the chord along the span, the angle of attack, and the slope of the curve of normal force for each section. Also, the nearer a section is to the tip the greater is its importance, because of its longer moment arm and the larger difference in angle of attack between it and the mid-span section when the wing is rolling. With these points in mind, the following ways may be noted by which the relative variation in wing-section loads with angle of attack may be influenced:

1. Change in profile along the span.
2. Twist.
3. Sweepback.
4. Taper in plan form.

The present investigation was undertaken for the purpose of obtaining information concerning the extent to which lateral stability in roll, both above and below the stall, could be affected by changing the shape of a monoplane wing according to three of the above methods: change in profile along the span, twist, and sweepback. Tests were also made of combinations of change in profile along the span with twist or sweepback to obtain information on the possible variation in the characteristics due to the latter variables with change in wing profile. All the tests were made in the 5-foot, closed-throat atmospheric wind tunnel of the Langley Memorial Aeronautical Laboratory. (Reference 1.)

The distribution of the loads normal to the chord along the span is used as the basis of analysis. These loads were obtained by using the pressure-distribution method of test.

MODELS AND APPARATUS

It has been standard practice in pressure-distribution investigations in the atmospheric wind tunnel to make the assumption that there is no flow of air across the plane of symmetry of an unyawed, full-span wing. The further assumption follows that an actual surface
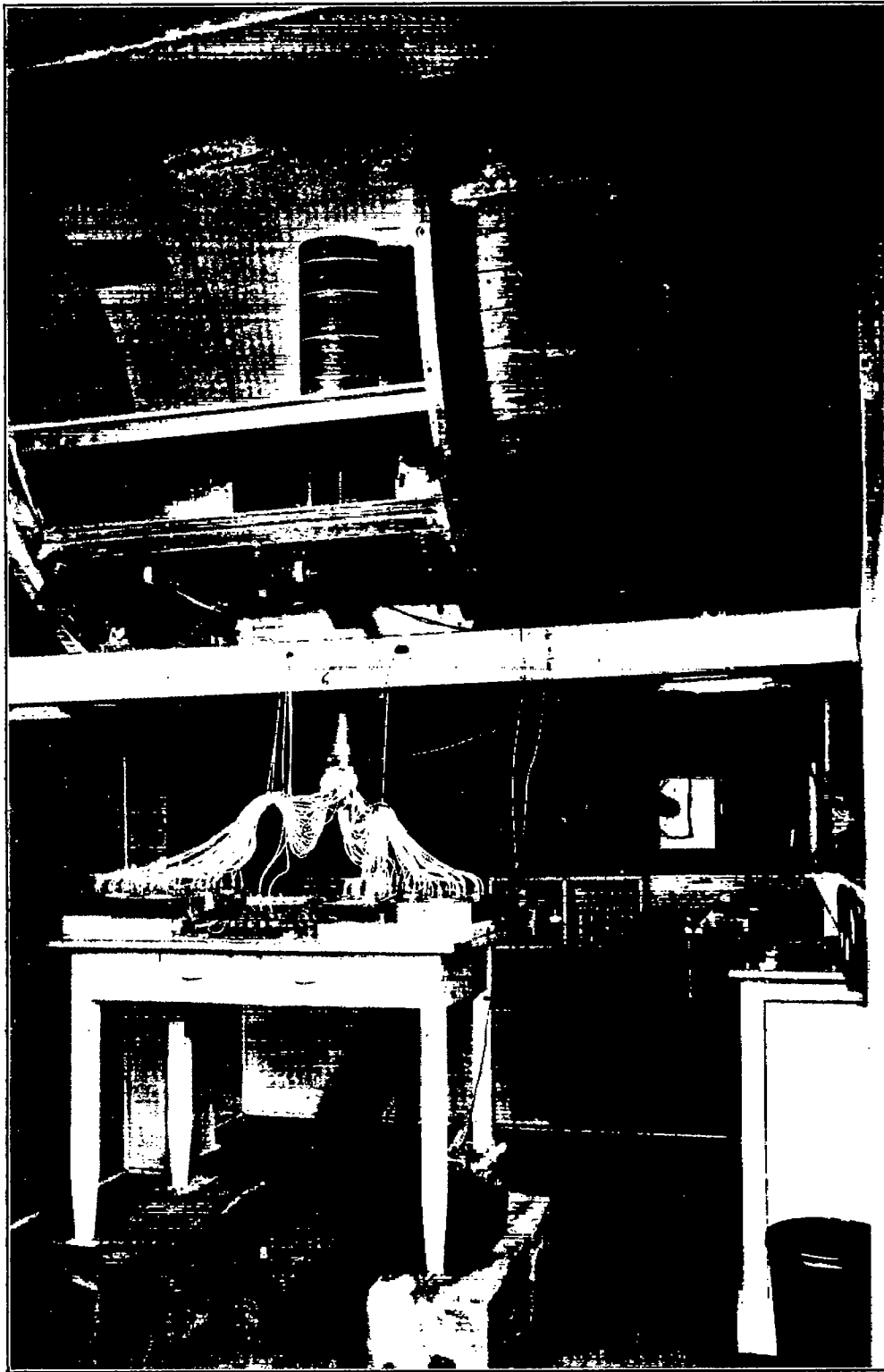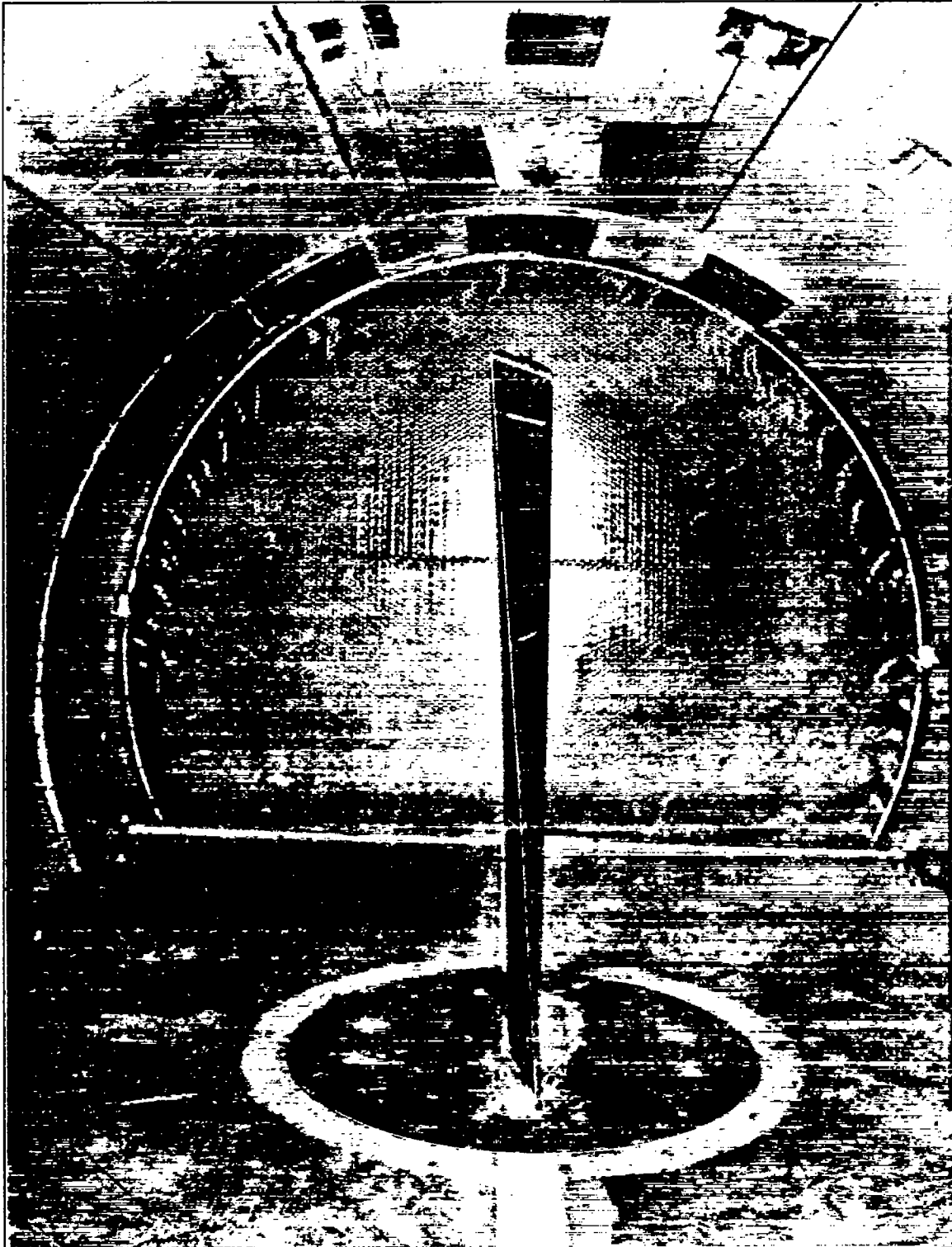
FIGURE 1.—General view of test apparatus

FIGURE 2.—Wing model mounted on separation plane

may be located in this plane without seriously affecting the air flow over either half of the wing. This makes it possible to omit one-half of the wing and test only a semispan model with a "separation" plane mounted in its plane of symmetry, as shown in Figures 1 and 2 and described in greater detail in reference 2.

The general design of the two semispan wing models and the locations of the test orifices are shown in Figure 3, and the profile ordinates in per cent of chord are given in Tables I and II. One wing model, designated the N. A. C. A. 84, is of constant profile and

instead of parallel to the span, and were held together by the clamping action of two long bolts instead of being rigidly glued together. This method of assembly was necessary in order to allow the wings to be given a maximum linear twist of either 15° washin or washout. Figure 2 shows the N. A. C. A. 84 model washed out 15° about an axis coincident with the leading edge.

In order to set the twist the long bolts were loosened and the laminations rotated through a small angle relative to each other until the trailing edge and a line
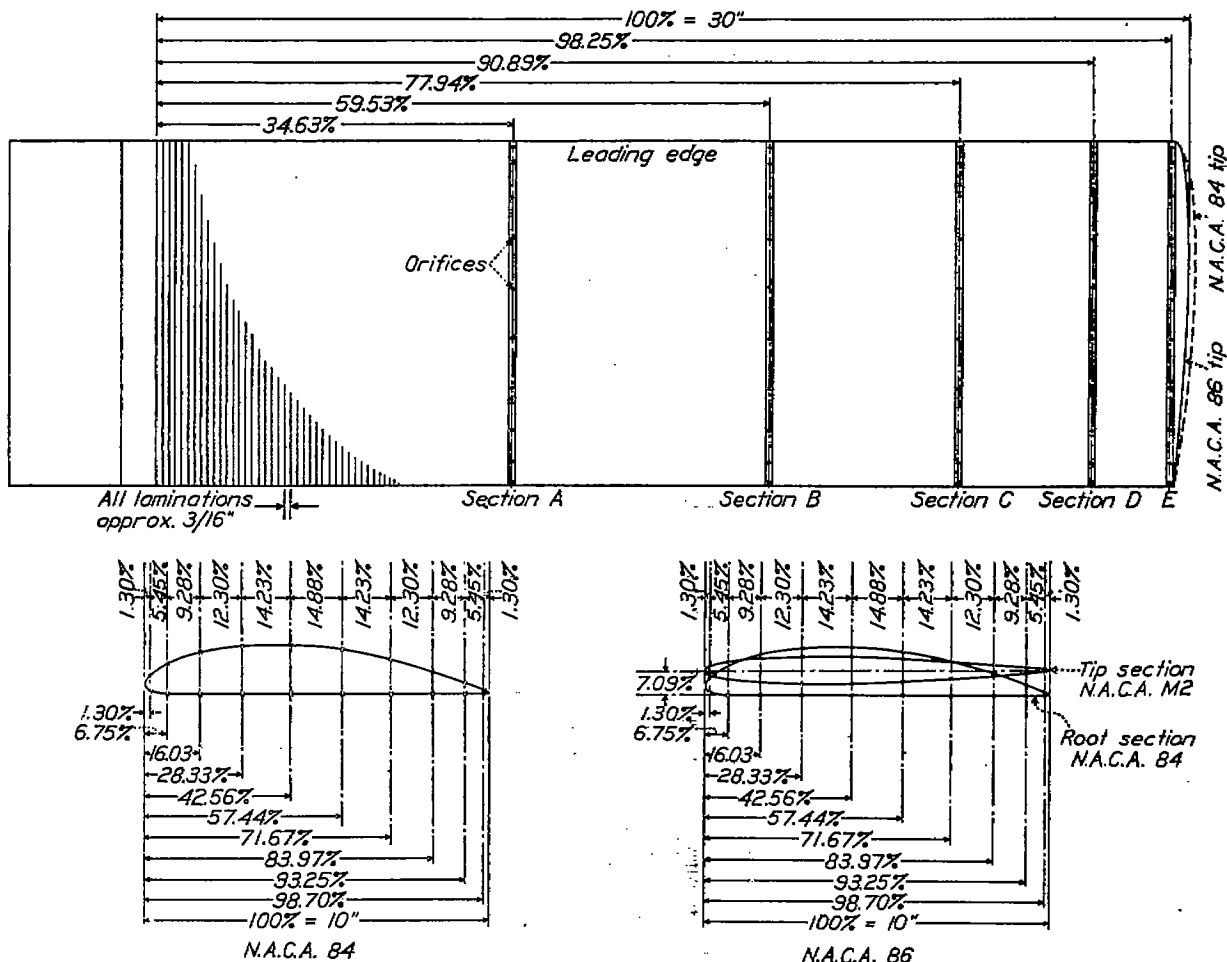

FIGURE 3.—Orifice locations on semispan twistable wing models

nated the N. A. C. A. 84, is of constant profile and thickness from the root to the tip pressure element. The other, the N. A. C. A. 86, tapers in thickness equally from the upper and lower surfaces from the N. A. C. A. 84 profile at the root to the N. A. C. A.-M2 symmetrical profile at the tip pressure element. Slightly beyond this section the plan forms of both wings depart from rectangular to form a rounded tip of such shape that any section normal to the mean camber line is a semicircle whose diameter is the wing thickness at that section.

The construction of the two wing models differed from conventional pressure-distribution design in that the laminations were placed parallel to the chord

scribed on the leading edge of the model coincided with their calculated projections marked on a twist-jig.

Sweepback was obtained by loosening the mounting clamp, seen just under the separation plane in Figure 1, and rotating the entire wing about an axis in the plane of symmetry and normal to the midspan chord at its 50 per cent point.

A sheet-metal fairing was placed beneath the separation plane and around the mounting clamp to decrease the interference of the apparatus in the tunnel with the air stream. A torque tube extending out of the tunnel directly beneath the wing was connected to the mounting clamp and served as a means for changing the angle of attack. The brass pressure

tubes passed through the center of this member and were connected by short lengths of rubber tubing to an integrating multiple manometer on the table. A spot-light mounted on a bracket above the table furnished the light to expose the photostatic records obtained on the manometer.

Experience with pressure-distribution investigations in the past has demonstrated the need for reducing the labor involved in working up the test data. Since the object of the present investigation was primarily to study span-load distribution, a manometer was used that automatically integrated the section loads and thereby reduced the manual integration steps from six to one. A more complete discussion of the principle of operation and the design of this instrument is given in reference 3.

TESTS

Preliminary tests were conducted on the manometer as originally designed for use with mercury, but the results were unsatisfactory. Alcohol was substituted as a manometer liquid and the air speed was reduced from 117 feet per second to about 32 feet per second. At this speed the hydraulic heads encountered were within the structural limits of the manometer and satisfactory checks on repeat runs could be obtained.

A vertical dynamic-pressure survey, as shown in relation to the wing model in Figure 4, was made at an air speed of about 32 feet per second for the purpose of calibrating the Pitot-static tube which was used during the tests to indicate the air speed. This "service" Pitot tube was located several feet upstream and ahead of the honeycomb, where it was not influenced by the presence of the model.
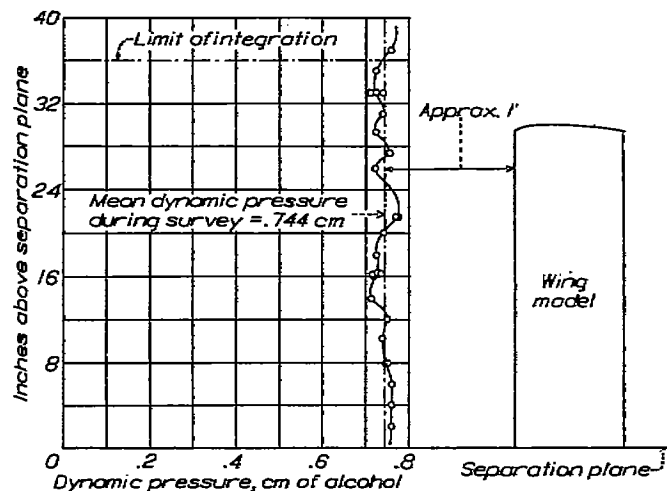

FIGURE 4.—Dynamic pressure distribution

The first test with the wing twisted was made at 15° washout. A check test was then made with the small "steps," caused by the laminations rotating past each other, faired over with plasticine. A small difference in the results was noted, and consequently all subsequent tests were made with the wing faired when twisted.

The test program for each wing was divided into three parts, as follows:
1. Straight wing (zero geometric twist).
2. Wing twisted with a uniform change in angle along the span to an angle at the tip equal to:
   (a) 5° washin.
   (b) 5°, 10°, and 15° washout.
3. Sweepforward, 10° and 20°; sweepback, 10° and 20°.

Each wing condition was tested at angles of attack from −9° to +30° at 3-degree intervals, conventional pressure-distribution test procedure being employed.

The dynamic pressure was maintained constant at 1.23 pounds per square foot, corresponding to an air speed of 32.3 feet per second in standard air and a Reynolds Number of about 160,000.

RESULTS

The results of this investigation are presented graphically in Figures 5 to 20; critical values of the rolling moment and normal-force coefficients are also given in Table III. Complete section and total wing normal-force data are given in Tables IV to XXI.

The coefficient of rolling moment due to roll C_λ about the wind axis, is plotted against absolute angle of attack in Figures 5, and 8 to 15. Although the rolling moments as given are not about the probable axis of rotation of an airplane in flight, the wind axis was chosen for convenience in the comparison of the computed moments with autorotation test moments, which are always taken about the wind axis. This method of presentation allows all wing settings to be compared on a basis of equal angular displacement from zero lift, and all numerical values of C_λ, with corresponding autorotation results. The use of the wind axis instead of the body axis, which is nearer to the true axis of roll, does not affect the relative value of the results appreciably.

The computation of C_λ is based on the strip theory (reference 4), assuming a rate of rotation such that

$$\frac{pb}{2V} = 0.05$$

In this expression
p = rate of rotation in roll (radians per second),
b = span of the wing (feet),
V = air speed (feet per second).

The numerical value 0.05 corresponds to the maximum rolling velocity found to be encountered in ordinary flight in bumpy air. The numerical value of C_λ is obtained from the equation

$$C_\lambda = \frac{\lambda}{qbS} \cos \alpha$$

where
> λ = total rolling moment due to the unsymmetrical distribution of forces normal to the chord,
> α = angle of attack of wing root,
> q = dynamic pressure,

and S = area of the wing.
Positive values of C_λ indicate a moment tending to aid the assumed rotation and negative values indicate a moment opposing it. Where $C_\lambda = 0$, it is obvious that neutral equilibrium exists.

Curves of the asymmetric normal load along the span used in the computation of C_λ were derived from section normal-force curves such as are given in Figures 6 and 7. The values of C_N' shown here and those for the other wing settings presented in the tables were computed by multiplying the results obtained on the integrating manometer by a constant depending upon the manometer design.

The normal-force coefficient of the whole wing C_N, as shown in Figures 16 to 20, was obtained by plotting C_N' against span and graphically integrating for total normal force. Reduction of these integrals to nondimensional form gave the coefficient

$$C_N = \frac{N}{qS}$$

where N = total normal force.

It should be borne in mind, in applying these results to a full-scale wing, that the Reynolds Number of the tests was 160,000 and no corrections have been made to compensate for the lack of free-air conditions in the tunnel. In both respects, however, the results are directly comparable to those of numerous other investigations in this wind tunnel.

Attention is also drawn to the conclusion arrived at in reference 5 relative to the shape in front elevation of the extreme wing-tip fairing. This indicates that the stability of a wing with such a faired tip is likely to be less and its instability greater than one with a purely rectangular tip. However, since the models used in this investigation had geometrically similar tips, the difference between them due to this effect is considered unimportant.

The accuracy of the results, as plotted, may be considered to be within ± 5 per cent as explained in detail in the following paragraphs. The occasional points at negative lift that were omitted on the curves were seriously in error, owing to the failure of the manometer always to function properly under this type of loading. Test conditions were maintained to the following accuracies: mean dynamic pressure, ± 1 per cent; and the setting of the angles of attack, twist, and sweepback, ± 5 minutes.

The rolling-moment coefficient C_λ, as calculated on the strip method basis from semispan pressure-dis-

tribution tests, is useful for the purpose of comparing wings tested under similar conditions. However, the absolute values of the coefficient will differ from those that would be obtained from full-span wings or tests in which the wing would be given a small angular velocity in roll. Comparative tests indicating the amount of this difference at the very low rate of roll used are lacking. However, since the accuracy of the strip method increases as the rate of rotation approaches zero, the inherent error in the results due to the method of calculation is considered to have an unimportant influence. The error due to the semispan method of test is considered negligible considering the large distance from the separation plane to the first row of pressure orifices.

The numerical error of most importance in the computation of C_λ is probably to be found in the fairing of the section curves of normal force against angle of attack and the accuracy of determination of the points through which they are drawn. The error due to the former is not directly estimable, but is believed to be small. The average deviation of the latter throughout two check runs amounted to about 3½ per cent of the mean observed value. As will be seen from Figures 6 and 7, small vertical errors in the plotted points would not greatly change the slopes of the curves in most cases. As the determination of the asymmetric normal forces and the integration of the resulting rolling-force curves were each accurate to within 1 per cent, an average deviation of not more than ± 5 per cent could be expected in the plotted values of C_λ.

The greatest source of error believed to enter into the normal-force results is in fairing the semispan load curves from the pressure element nearest the root to the root. This error depends upon the judgment of the individual doing the fairing and upon the accuracy of the last measured point. Check runs showed that the variation of this point was less than 2 per cent of its mean value. Consequently the areas of the measured semispan load curves probably do not deviate from the actual load curves more than ± 5 per cent, and the coefficient of normal force may be considered accurate to that extent.

DISCUSSION

From the viewpoint of lateral stability it is important to consider the tendency of a wing system to increase or damp a small rotation in roll when the moment causing the rotation ceases. The coefficient of rolling moment due to roll C_λ taken at a rate of rotation equivalent to the maximum usually encountered by an airplane flying in bumpy weather $\left(\frac{pb}{2V} = 0.05\right)$, provides a convenient measure of this tendency. Figures 5 and 8 to 15 give curves of C_λ under the above con-

ditions and may, therefore, be considered as indicating the degree of initial lateral stability or instability of each wing arrangement in normal, unyawed flight.

In studying these curves, it should be borne in mind that varying the profile along the span from a cambered to a symmetrical section is, in effect, a method of producing an "equivalent twist." In the case of the N. A. C. A. 86 airfoil as compared to the N. A. C. A. 84, this "equivalent twist" is approximately equal to 7° washout, or the difference in angle of zero lift of the root and tip sections.

Figure 5 shows the effect on rolling moment due to roll of such a change in profile along the span. The most striking effect is the reduction in the magnitude of maximum instability, which for the N. A. C. A. 86 wing model is about one-sixth of that for the N. A. C. A. 84. An explanation of this phenomenon may be obtained by reference to Figures 6 and 7, where a marked difference in the shapes of the section normal-force curves for the two wings is seen. In the vicinity of 23° (30° absolute angle of attack) where lateral instability is the greatest for the N. A. C. A. 84 wing, the slopes of all its section curves are distinctly negative. On the other hand, the section surves for the N. A. C. A. 86 at about 15° (18½° absolute angle of

FIGURE 5.—Effect of variation in profile along the span on rolling moment due to roll at $\frac{pb}{2V}=0.05$

attack) have a slope which is negative for about half of the semispan, then zero, and finally strongly positive at the tip. The greater influence on lateral stability of the tip sections, whose stalling angles on this wing are considerably delayed, would account for the very great improvement in stability over the N. A. C. A. 84 wing.

However, the N. A. C. A. 86 has the disadvantage that lateral instability first appears at a lower absolute angle of attack by 10° than that at which it appears

on the N. A. C. A. 84 wing. This condition may be considered mainly a function of the characteristics of the intermediate profiles, because twist on the N. A. C. A. 84 equal to the equivalent twist of the

FIGURE 6.—N. A. C. A. 84 straight wing. Section normal force versus angle of attack

FIGURE 7.—N. A. C. A. 86 straight wing. Section normal force versus angle of attack

N. A. C. A. 86 straight wing (as interpolated from Figure 8) reduces the angle of attack of neutral stability only about 2°.

Geometric twist has the effects shown in Figures 8 and 9. It is seen that the good lateral stability

characteristics of the N. A. C. A. 86 wing are improved by a small amount of washout and are not materially impaired by additional washout up to 10°. In Figure 10 maximum lateral instability is plotted against equivalent twist for both wings. This shows that an equivalent twist in the order of 11° washout is apparently the maximum desirable for both wings from the standpoint of lateral instability due to roll. The similarity of the two curves for like amounts of

maximum normal force and the beginning of lateral instability is very small for both wings and may be considered practically c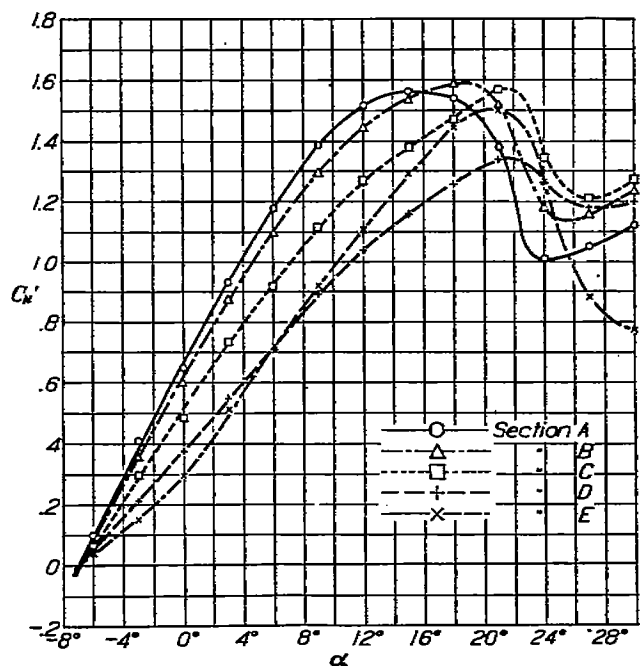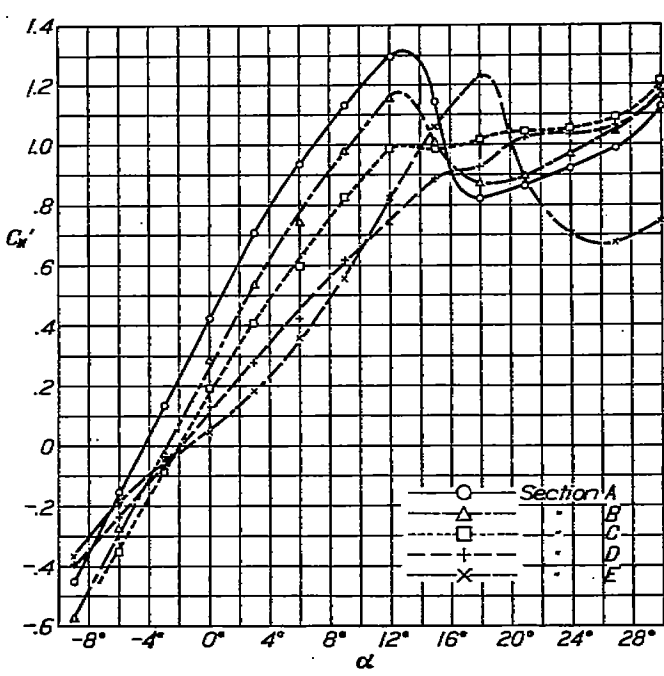oincident if less than a degree. The unusually large difference occurring at zero twist of the N. A. C. A. 84 is probably due to the very rounded top to the normal force curve of this wing, as compared to its twisted variations. (Fig. 17.)

The influence of sweepback on the lateral stability of the two wing models is shown in Figures 12 to 15.

FIGURE 8.—N. A. C. A. 84 airfoil. Effect of twist on rolling moment due to roll at

$$\frac{pb}{2V}=0.05$$

FIGURE 10.—Maximum lateral instability versus equivalent twist

NOTE.—Figures at points on N. A. C. A. 86 curve indicate degrees of geometric twist.
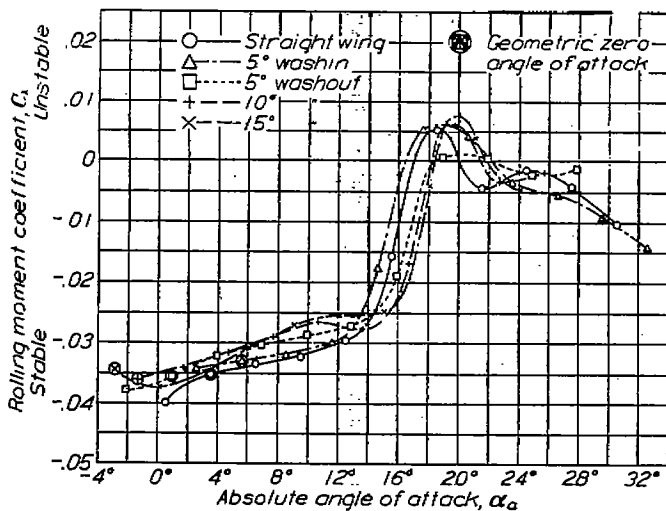
FIGURE 9.—N. A. C. A. 86 airfoil. Effect of twist on rolling moment due to roll at

$$\frac{pb}{2V}=0.05$$
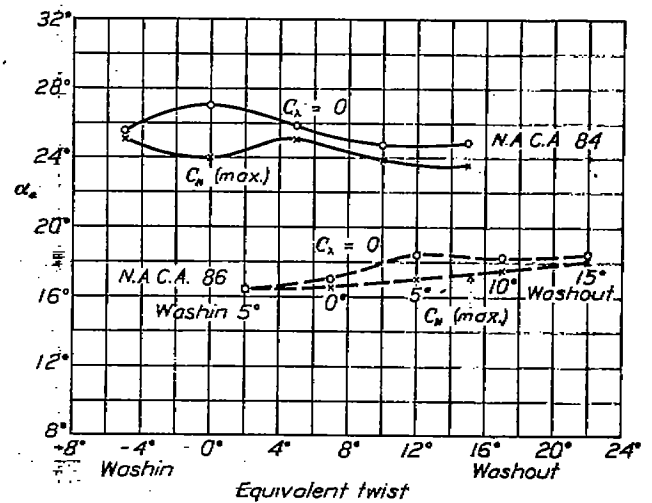
FIGURE 11.—Absolute angle of attack of neutral stability and maximum normal force versus equivalent twist

NOTE.—Figures at points on N. A. C. A. 86 curve indicate degrees of geometric twist.

twist is fair, both showing a reduction due to twist of at least 70 per cent in maximum unstable rolling moment.

The absolute angle of attack of initial neutral stability and of maximum normal force plotted against equivalent twist is shown in Figure 11. The variation is small for each wing and within the range of the tests the N. A. C. A. 84 always shows instability beginning at a higher absolute angle of attack than the N. A. C. A. 86. The angular difference between

Sweepforward is seen to raise the angle of attack of neutral stability and sweepback to lower it, relative to the angle for the straight wing. This effect seems to be due to the fact that the tips, which affect lateral stability more than any other part of the wing, act in a manner analogous to the leading edge of an airfoil when swept forward and the trailing edge when swept back. Thus, in the former case, the slopes of the normal-force curves for the tip sections are increased and their maxima delayed, both of which tend to maintain lateral

stability to a higher angle of attack. When the wing is swept back the slopes are decreased and their maximum points occur at lower angles, which has the opposite effect upon the angle of neutral lateral stability.

On the other hand, Figure 15 also shows that the influence of the above condition on the angle of maximum normal force is to raise the angle slightly for both sweepforward and sweepback. This condition
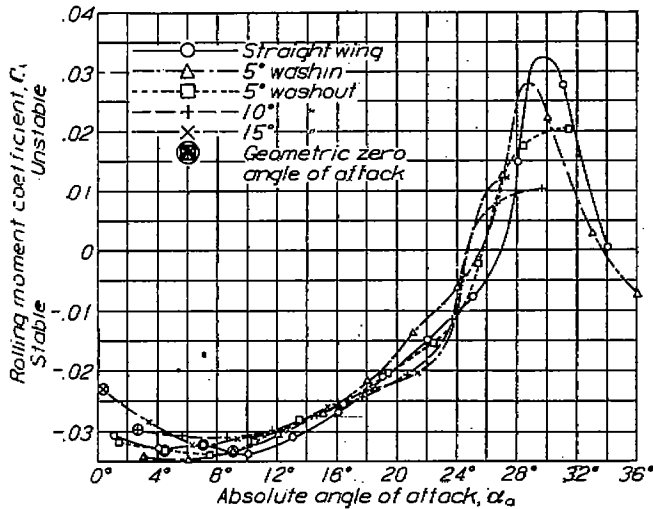

FIGURE 12.—N. A. C. A. 84 airfoil. Effect of sweepback on rolling moment due to roll at $\frac{pb}{2V}=0.05$
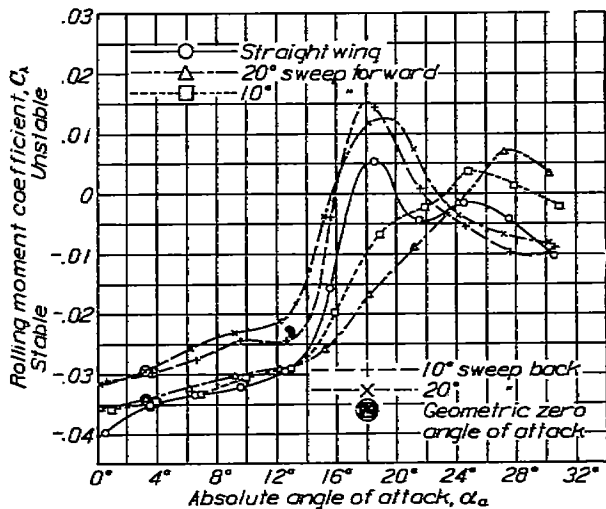
FIGURE 13.—N. A. C. A. 86 airfoil. Effect of sweepback on rolling moment due to roll at $\frac{pb}{2V}=0.05$

produces, at 20° sweepback, a definite tendency towards lateral instability before the stall.

Little similarity in the maximum instability characteristics of the two wings can be observed, which indicates that the effect of sweepback is appreciably influenced by the obviously very different thickness of the extreme tips of the two wings.

For more convenient numerical comparison, the critical values of the foregoing curves (as shown in figs. 10, 11, 14, and 15) and the maximum normal-force coefficient for each wing arrangement are tabulated below.

Curves of total normal-force coefficient C_N against angle of attack are given in Figures 16 to 20 for the purpose of showing the effect of the variables used to change the span-load distribution upon the general effectiveness of the wings tested. It is realized that the absence of data on the changes in drag accompanying the changes in normal-force distribution makes a complete comparison impossible. However, the close

FIGURE 14.—Maximum lateral instability versus sweepback
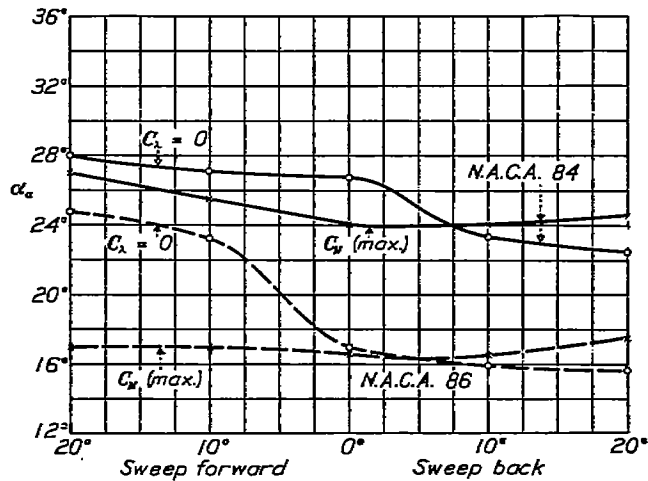
FIGURE 15.—Absolute angle of attack of neutral lateral stability and maximum normal force versus sweepback

approximation of normal force to the lifting force justifies the use of C_N for this purpose.

The effect of change in profile is shown in Figure 16. Maximum C_N is reduced 12 per cent and the abruptness of the stall is considerably increased. The angle of attack of zero lift is increased by the amount that might be expected from the equivalent washout of the tip of the N. A. C. A. 86 wing. As mentioned before, the angle of attack of neutral lateral stability (approximately maximum C_N) is decreased, which results in a decrease of over 8° in the available flying range. Thus, though the straight N. A. C. A. 86 wing shows a

marked reduction in lateral instability (fig. 5), it is distinctly inferior to the N. A. C. A. 84 in other respects.
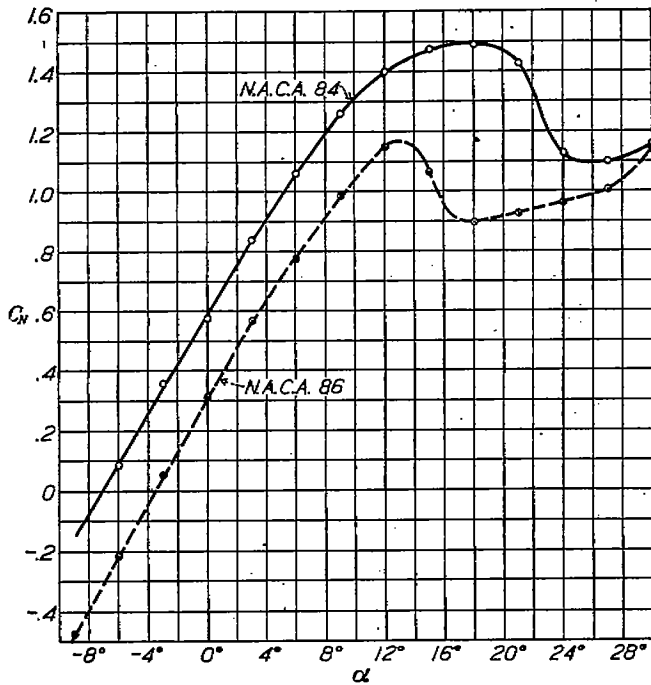
FIGURE 16.—Total normal force versus angle of attack. Effect of change in profile from N. A. C. A. 84 at root to N. A. C. A.–M2 at tip

TABLE III

MAXIMUM LOADS AND MOMENTS AND CRITICAL ANGLES OF ATTACK

α_s=angle of attack above zero lift.
+Twist=washin.
−Twist=washout.
+Sweepback=Sweepback
−Sweepback=sweepforward.

Wing characteristics			Max. C_A	Max. C_N	α_s at $C_A=0$	α_s at C_N (Max.)
Profile	Geometric twist	Sweepback				
	Degrees	*Degrees*			*Degrees*	*Degrees*
N. A. C. A. 84	0	0	0.0323	1.490	27.0	24.0
	+5	0	.0279	1.471	26.5	25.0
	−5	0	.0202	1.500	25.8	25.0
	−10	0	.0102	1.420	24.7	23.7
	−15	0	.0120	1.418	24.8	23.5
	0	−20	.0220	1.485	28.0	27.0
	0	−10	.0340	1.485	27.1	26.5
	0	10	.0246	1.380	23.2	24.0
	0	20	.0199	1.380	22.5	24.5
N. A. C. A. 86	0	0	.0052	1.168	17.0	16.5
	+5	0	.0062	1.110	16.4	16.5
	−5	0	.0013	1.140	18.4	17.0
	−10	0	.0062	1.159	18.2	17.5
	−15	0	.0076	1.153	18.4	18.0
	0	−20	.0071	1.171	24.7	17.0
	0	−10	.0038	1.165	23.8	17.0
	0	10	.0153	1.078	15.9	16.5
	0	20	.0125	1.031	15.6	17.5

Twist, as shown in Figures 17 and 18, makes very little change in the value of C_N maximum of either wing. In the case of the N. A. C. A. 84, washout increases the abruptness of the stall, whereas the

N. A. C. A. 86 shows a decrease for washin and no change for washout. Zero lift for both wings in nearly all cases is shifted slightly less than might be expected.

The effect of sweep is shown in Figures 19 and 20. Sweepforward has no effect on the magnitude of C_N
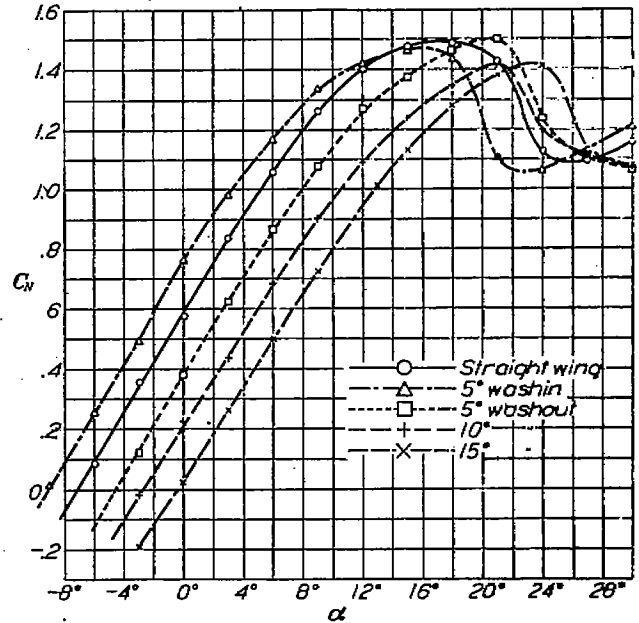
FIGURE 17.—N. A. C. A. 84 airfoil. Total normal force versus angle of attack. Effect of twist
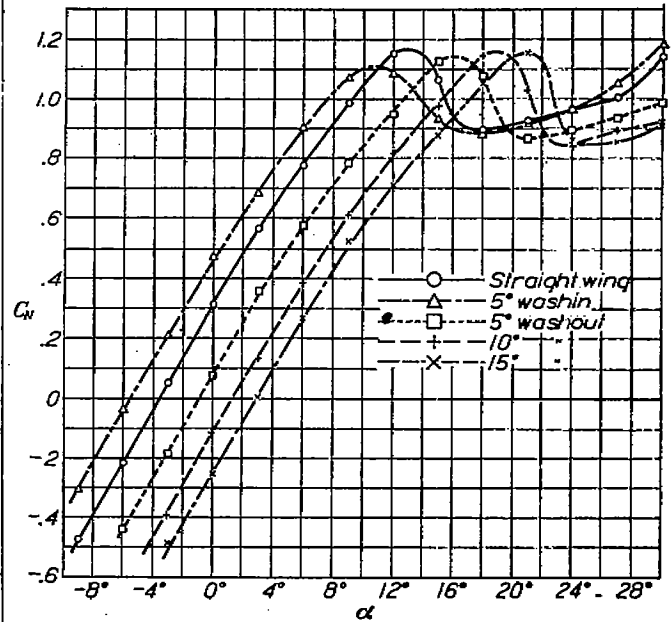
FIGURE 18.—N. A. C. A. 86 airfoil. Total normal force versus angle of attack. Effect of twist

maximum of either wing. Sweepback, on the other hand, gives a uniform reduction in C_N maximum of 7½ per cent for the N. A. C. A. 84, and a progressive decrease in C_N maximum for the N. A. C. A. 86 amounting to 12 per cent at 20°. The angle of attack of zero lift for either wing is not affected by sweepforward or sweepback to any appreciable extent.
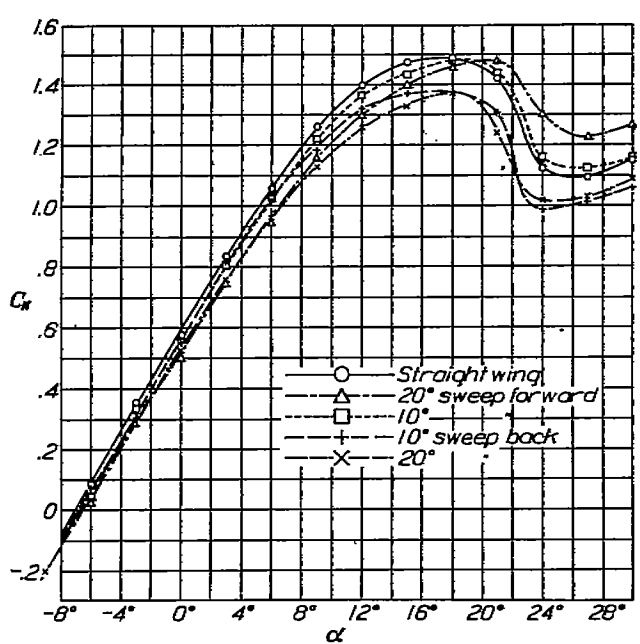
FIGURE 19.—N. A. C. A. 84 airfoil. Total normal force versus angle of attack.
Effect of sweep
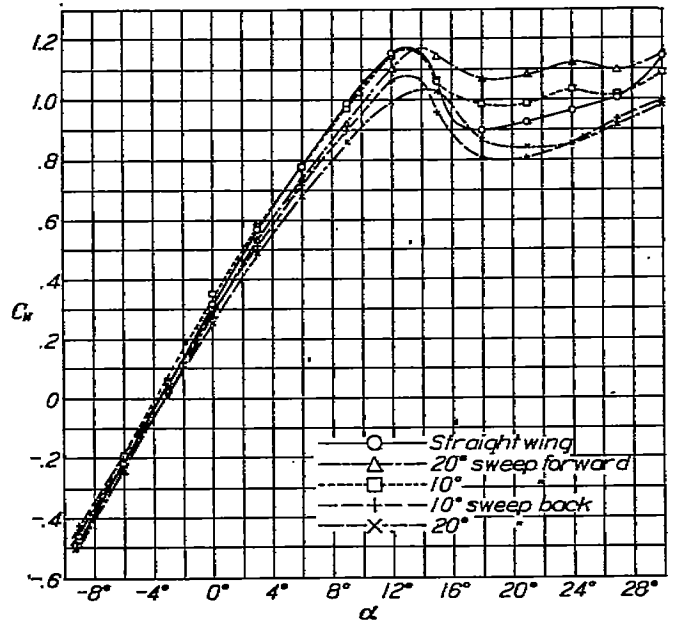
FIGURE 20.—N. A. C. A. 86 airfoil. Total normal force versus angle of attack.
Effect of sweep

CONCLUSIONS

The span-load distributions obtained in these tests show the following effects on lateral instability as governed by rolling moment due to roll:

1. Variation in profile of an airfoil from the N. A. C. A. 84 section at the root to the N. A. C. A.–M2 at the tip reduces maximum instability to about one-sixth of that of an airfoil of constant N. A. C. A. 84 profile.

2. About 11° equivalent washout reduces maximum instability about 75 per cent.

3. Sweepforward raises the angle of neutral stability, while sweepback reduces it. This effect is of sufficient magnitude so that at 20° sweepback instability begins before the wing reaches maximum lift.

The various span-load distributions tested influence the general effectiveness of the wings to the following extent:

1. The variation in profile along the span reduces the useful angle-of-attack range about 37 per cent and maximum C_N about 12 per cent.

2. Twist has only a slight influence on the useful angle-of-attack range and maximum C_N.

3. Transition from sweepforward to sweepback progressively decreases the useful angle-of-attack range.

4. Sweepforward up to 20° has no effect on maximum C_N and sweepback up to 20° reduces it about 10 per cent.

LANGLEY MEMORIAL AERONAUTICAL LABORATORY,
NATIONAL ADVISORY COMMITTEE FOR AERONAUTICS,
LANGLEY FIELD, VA., *March 4, 1931*

REFERENCES

1. Reid, Elliott G.: Standardization Tests of N. A. C. A. No. 1 Wind Tunnel. N. A. C. A. Technical Report No. 195, 1924.
2. Reid, Elliott G.: Pressure Distribution Over Thick, Tapered Airfoils, N. A. C. A. 81, U. S. A. 27C Modified, and U. S. A. 35. N. A. C. A. Technical Report No. 229, 1926.
3. Noyes, Richard W.: An Integrating Manometer for use in Wind Tunnel Pressure Distribution Measurements. N. A. C. A. Technical Note No. 377, 1931.
4. Knight, Montgomery: Wind Tunnel Tests on Autorotation and the "Flat Spin." N. A. C. A. Technical Report No. 273, 1927.
5. Rhode, Richard V. and Lundquist, Eugene E.: The Pressure Distribution Over a Square Wing Tip on a Biplane in Flight. N. A. C. A. Technical Note No. 360, 1931.

TABLE I
N. A. C. A. 84
PROFILE ORDINATES

Station, % chord from L. E.	Upper surface, % chord	Lower surface, % chord
0	2.50	2.50
1.25	4.85	.95
2.50	6.05	.41
5.00	7.78	.10
7.50	9.03	.02
8.50	----	.00
10.00	10.00	.00
15.00	11.50	.00
20.00	12.71	.00
25.00	13.51	.00
30.00	14.00	.00
35.00	14.18	.00
40.00	14.11	.00
50.00	13.50	.00
60.00	12.31	.00
70.00	10.32	.00
80.00	7.71	.00
90.00	4.39	.00
95.00	2.41	.00
100.00	.30	.00

TABLE II
N. A. C. A. -M2
PROFILE ORDINATES

Station, % chord from L. E.	Upper surface, % chord	Lower surface, % chord
0	0	0
1.25	1.30	-1.30
2.50	1.74	-1.74
5.00	2.33	-2.33
7.50	2.74	-2.74
10.00	3.05	-3.05
15.00	3.49	-3.49
20.00	3.78	-3.78
30.00	4.03	-4.03
40.00	4.00	-4.00
50.00	3.74	-3.74
60.00	3.30	-3.30
70.00	2.71	-2.71
80.00	1.99	-1.99
90.00	1.15	-1.15
95.00	.69	-.69
100.00	.20	-.20

TABLE IV
N. A. C. A. 84
STRAIGHT WING
NORMAL-FORCE COEFFICIENTS

α	C_N' Sec. A	Sec. B	Sec. C	Sec. D	Sec. E	C_N total wing
Degrees						
-6	0.097	0.038	0.058	0.055	0.045	0.083
-3	.409	.358	.296	.211	.149	.354
0	.650	.598	.484	.373	.293	.576
3	.929	.875	.734	.546	.510	.835
6	1.176	1.096	.916	.718	.719	1.059
9	1.384	1.291	1.111	.890	.917	1.250
12	1.511	1.440	1.267	1.037	1.105	1.400
15	1.559	1.534	1.378	1.154	1.287	1.475
18	1.538	1.586	1.455	1.255	1.440	1.489
21	1.375	1.517	1.564	1.339	1.495	1.424
24	1.006	1.173	1.340	1.258	1.260	1.126
27	1.046	1.153	1.204	1.177	.877	1.098
30	1.118	1.233	1.265	1.194	.770	1.152

TABLE V
N. A. C. A. 84
5° WASHIN
NORMAL-FORCE COEFFICIENTS

α	C_N' Sec. A	Sec. B	Sec. C	Sec. D	Sec. E	C_N total wing
Degrees						
-9	-0.007	0.046	0.072	0.007	0.052	0.012
-6	.254	.312	.306	.176	.176	.253
-3	.533	.545	.507	.331	.332	.470
0	.825	.838	.741	.507	.520	.768
3	1.063	1.047	.942	.676	.761	.935
6	1.254	1.240	1.111	.840	.943	1.170
9	1.418	1.390	1.253	.989	1.151	1.338
12	1.490	1.470	1.365	1.119	1.365	1.420
15	1.520	1.390	1.430	1.230	1.554	1.463
18	1.462	1.307	1.500	1.288	1.612	1.439
21	.995	1.143	1.308	1.255	1.204	1.112
24	1.008	1.130	1.221	1.150	.962	1.062
27	1.072	1.195	1.274	1.176	.807	1.130
30	1.158	1.280	1.351	1.255	.793	1.210

TABLE VI
N. A. C. A. 84
5° WASHOUT
NORMAL-FORCE COEFFICIENTS

α	C_N' Sec. A	Sec. B	Sec. C	Sec. D	Sec. E	C_N total wing
Degrees						
-3	0.182	0.094	0.055	-0.032	0.016	0.121
0	.482	.393	.289	.104	.101	.378
3	.760	.634	.497	.279	.250	.523
6	1.008	.895	.725	.435	.433	.866
9	1.222	1.115	.920	.605	.647	1.073
12	1.424	1.310	1.095	.761	.847	1.269
15	1.520	1.440	1.260	.910	.990	1.374
18	1.565	1.545	1.381	1.063	1.206	1.466
21	1.551	1.609	1.435	1.178	1.330	1.500
24	1.072	1.412	1.530	1.202	1.343	1.235
27	1.000	1.128	1.303	1.197	1.225	1.100
30	1.040	1.140	1.148	1.040	.913	1.063

TABLE VII
N. A. C. A. 84
10° WASHOUT
NORMAL-FORCE COEFFICIENTS

α	C_N' Sec. A	Sec. B	Sec. C	Sec. D	Sec. E	C_N total wing
Degrees						
-3	0.039	-0.059	-0.110	-0.202	-0.156	-0.020
0	.338	.149	.045	-.039	-.020	.227
3	.585	.416	.227	.084	.097	.434
6	.885	.663	.448	.247	.221	.638
9	1.091	.903	.663	.396	.384	.902
12	1.300	1.125	.839	.572	.572	1.090
15	1.430	1.295	1.000	.709	.780	1.238
18	1.515	1.419	1.150	.852	1.015	1.345
21	1.555	1.548	1.287	1.015	1.139	1.420
24	1.157	1.502	1.340	1.072	1.105	1.198
27	1.020	1.312	1.305	1.130	1.118	1.113
30	1.015	1.118	1.197	1.118	1.021	1.075

TABLE VIII
N. A. C. A. 84
15° WASHOUT
NORMAL-FORCE COEFFICIENTS

α	C_N'					C_N total wing
	Sec. A	Sec. B	Sec. C	Sec. D	Sec. E	
Degrees						
-3	-0.123	-0.214	-0.273	-0.377	-0.273	-0.190
0	.123	-.082	-.130	-.221	-.136	.024
3	.430	.163	.000	-.058	-.058	.256
6	.695	.455	.189	.046	.072	.496
9	.962	.702	.417	.208	.188	.726
13	1.242	1.020	.702	.435	.403	1.012
15	1.384	1.157	.820	.540	.533	1.131
18	1.495	1.313	.987	.682	.722	1.280
21	1.572	1.450	1.130	.825	.916	1.382
24	1.548	1.548	1.300	1.008	1.060	1.413
27	1.048	1.405	1.307	1.034	1.065	1.132
30	1.008	1.125	1.296	1.086	1.086	1.080

TABLE IX
N. A. C. A. 84
20° SWEEPFORWARD
NORMAL-FORCE COEFFICIENTS

α	C_N'					C_N total wing
	Sec. A	Sec. B	Sec. C	Sec. D	Sec. E	
Degrees						
-9	-0.130	-0.195	-0.195	-0.117	-0.383	-0.161
-6	.039	.020	.013	.046	-.123	.034
-3	.319	.280	.228	.202	.182	.294
0	.558	.494	.423	.357	.435	.505
3	.820	.740	.630	.507	.748	.752
6	1.036	.936	.813	.676	1.072	.950
9	1.254	1.131	.988	.845	1.350	1.161
12	1.371	1.289	1.162	.995	1.638	1.302
15	1.430	1.430	1.305	1.162	1.975	1.401
18	1.410	1.525	1.470	1.320	2.340	1.462
21	1.312	1.625	1.586	1.510	2.590	1.485
24	1.080	1.307	1.510	1.515	2.660	1.305
27	1.080	1.230	1.305	1.404	2.340	1.230
30	1.140	1.260	1.320	1.390	2.345	1.270

TABLE X
N. A. C. A. 84
10° SWEEPFORWARD
NORMAL-FORCE COEFFICIENTS

α	C_N'					C_N total wing
	Sec. A	Sec. B	Sec. C	Sec. D	Sec. E	
Degrees						
-6	0.053	0.046	0.026	0.046	-0.058	0.045
-3	.370	.338	.273	.208	.156	.332
0	.630	.572	.468	.364	.396	.563
3	.872	.820	.659	.546	.670	.803
6	1.118	1.040	.871	.722	.969	1.020
9	1.326	1.222	1.054	.878	1.222	1.218
12	1.444	1.335	1.216	1.015	1.535	1.368
15	1.509	1.495	1.359	1.157	1.820	1.438
18	1.495	1.560	1.483	1.300	2.055	1.485
21	1.340	1.625	1.580	1.430	2.127	1.440
24	.982	1.157	1.405	1.340	2.100	1.160
27	1.027	1.164	1.203	1.223	1.547	1.125
30	1.085	1.229	1.255	1.235	1.131	1.153

TABLE XI
N. A. C. A. 84
10° SWEEPBACK
NORMAL-FORCE COEFFICIENTS

α	C_N'					C_N total wing
	Sec. A	Sec. B	Sec. C	Sec. D	Sec. E	
Degrees						
-6	0.084	0.065	0.020	0.032	0.039	0.071
-3	.370	.351	.260	.195	.065	.327
0	.637	.611	.488	.358	.104	.555
3	.917	.878	.728	.520	.169	.819
6	1.151	1.086	.910	.670	.234	1.020
9	1.333	1.261	1.073	.813	.364	1.184
12	1.470	1.391	1.210	.943	.481	1.321
15	1.521	1.411	1.294	1.021	.578	1.377
18	1.521	1.300	1.281	1.073	.644	1.377
21	1.417	1.164	1.249	1.079	.624	1.309
24	1.027	.976	.982	.976	.345	.989
27	1.021	1.047	1.073	1.008	.403	1.018
30	1.066	1.112	1.125	1.040	.396	1.060

TABLE XII
N. A. C. A. 84
20° SWEEPBACK
NORMAL-FORCE COEFFICIENTS

α	C_N'					C_N total wing
	Sec. A	Sec. B	Sec. C	Sec. D	Sec. E	
Degrees						
-9	-0.266	-0.183	-0.104	-0.078	-0.039	-0.203
-6	.039	.020	.013	.006	.006	.036
-3	.332	.292	.247	.156	.019	.293
0	.592	.560	.487	.338	.026	.529
3	.850	.805	.720	.494	.045	.756
6	1.080	1.014	.890	.624	.032	.960
9	1.290	1.210	1.066	.760	.045	1.130
12	1.422	1.332	1.170	.851	.053	1.260
15	1.520	1.361	1.210	.897	.078	1.330
18	1.612	1.340	1.164	.897	.078	1.380
21	1.495	1.125	1.000	.835	.117	1.241
24	1.157	.943	.858	.805	.143	1.020
27	1.157	.981	.897	.818	.182	1.030
30	1.196	1.040	.943	.865	.280	1.090

TABLE XIII
N. A. C. A. 86
STRAIGHT WING
NORMAL-FORCE COEFFICIENTS

α	C_N'					C_N total wing
	Sec. A	Sec. B	Sec. C	Sec. D	Sec. E	
Degrees						
-9	-0.453	-0.573	-0.553	-0.394	-0.363	-0.474
-6	-.156	-.275	-.352	-.238	-.193	-.219
-3	+.132	-.025	-.060	-.074	-.047	.050
0	.424	+.268	+.193	+.128	.044	.313
3	.710	.533	.407	.274	.180	.567
6	.937	.743	.598	.423	.353	.776
9	1.133	.981	.826	.618	.554	.987
12	1.294	1.157	.988	.733	.825	1.152
15	1.114	1.012	.984	.867	1.058	1.063
18	.821	.576	1.017	.929	1.230	.898
21	.863	.897	1.043	1.023	.584	.924
24	.925	.973	1.052	1.036	.704	.962
27	.990	1.043	1.091	1.062	.680	1.006
30	1.128	1.170	1.214	1.175	.744	1.142

TABLE XIV
N. A. C. A. 86
5° WASHIN
NORMAL-FORCE COEFFICIENTS

α	C_N'					C_N total wing
	Sec. A	Sec. B	Sec. C	Sec. D	Sec. E	
Degrees						
−9	−0.331	−0.357	−0.318	−0.284	−0.156	−0.304
−6	−.025	−.071	−.078	−.065	−.025	−.033
−3	.246	.188	.175	.117	.058	.210
0	.538	.467	.389	.273	.201	.471
3	.778	.695	.583	.428	.389	.684
6	1.000	.902	.797	.623	.630	.905
9	1.168	1.096	.928	.780	.862	1.070
12	1.148	.980	.960	.862	1.110	1.088
15	.907	.810	.966	.850	1.062	.932
18	.842	.836	1.000	.971	.707	.885
21	.862	.907	1.025	1.011	.681	.923
24	.927	.972	1.077	1.042	.675	.970
27	1.032	1.076	1.153	1.120	.713	1.052
30	1.154	1.207	1.278	1.244	.790	1.185

TABLE XV
N. A. C. A. 86
5° WASHOUT
NORMAL-FORCE COEFFICENTS

α	C_N'					C_N total wing
	Sec. A	Sec. B	Sec. C	Sec. D	Sec. E	
Degrees						
−6	−0.396	−0.532	−0.570	−0.442	−0.473	−0.441
−3	−.104	−.272	−.337	−.272	−.266	−.191
0	.195	.013	−.117	−.117	−.091	.077
3	.484	.298	.143	.065	.006	.354
6	.746	.538	.350	.214	.104	.576
9	.960	.752	.545	.363	.266	.780
12	1.121	.945	.740	.532	.480	.948
15	1.290	1.150	.908	.668	.675	1.126
18	1.154	1.083	.966	.810	.843	1.075
21	.805	.921	1.000	.875	.972	.865
24	.830	.882	1.000	.920	1.142	.895
27	.907	.954	1.000	.960	.720	.933
30	.985	1.020	1.045	.992	.630	.983

TABLE XVI
N. A. C. A. 86
10° WASHOUT
NORMAL-FORCE COEFFICIENTS

α	C_N'					C_N total wing
	Sec. A	Sec. B	Sec. C	Sec. D	Sec. E	
Degrees						
−3	−0.285	−0.500	−0.538	−0.486	−0.518	−0.391
0	.032	−.234	−.344	−.285	−.305	−.113
3	.298	.032	−.130	−.143	−.117	.137
6	.577	.298	.117	.026	−.013	.386
9	.824	.545	.331	.175	.071	.609
12	1.039	.757	.519	.318	.214	.815
15	1.188	.965	.700	.467	.402	.978
18	1.350	1.148	.895	.648	.610	1.149
21	1.115	1.097	.934	.707	.714	1.030
24	.805	.920	.960	.817	.830	.848
27	.850	.894	.980	.882	1.000	.890
30	.922	.933	.955	.895	.760	.925

TABLE XVII
N. A. C. A. 86
15° WASHOUT
NORMAL-FORCE COEFFICIENTS

α	C_N'					C_N total wing
	Sec. A	Sec. B	Sec. O	Sec. D	Sec. E	
Degrees						
−8	−0.389	−0.565	−0.628	−0.655	−0.831	−0.436
0	−.091	−.402	−.532	−.493	−.545	−.256
3	.195	−.130	−.324	−.298	−.312	.002
6	.493	.155	−.071	−.135	−.123	.263
9	.760	.435	.168	.032	−.006	.524
12	.967	.660	.376	.195	.078	.710
15	1.129	.850	.557	.324	.203	.875
18	1.298	1.058	.740	.474	.389	1.053
21	1.355	1.200	.895	.622	.557	1.153
24	.868	1.039	.907	.660	.570	.804
27	.836	.927	.945	.771	.675	.857
30	.900	.915	.952	.815	.830	.912

TABLE XVIII
N. A. C. A. 86
20° SWEEPFORWARD
NORMAL-FORCE COEFFICIENTS

α	C_N'					C_N total wing
	Sec. A	Sec. B	Sec. C	Sec. D	Sec. E	
Degrees						
−9	−0.442	−0.552	−0.502	−0.422	−0.850	−0.484
−6	−.195	−.285	−.318	−.206	−.506	−.247
−3	.110	−.032	−.091	−.078	−.181	.026
0	.402	.234	.162	.104	.162	.264
3	.635	.460	.370	.285	.430	.530
6	.850	.642	.545	.441	.797	.733
9	1.020	.844	.758	.642	1.159	.920
12	1.194	1.043	.920	.700	1.501	1.100
15	1.104	1.101	1.110	.974	1.900	1.148
18	.895	1.149	1.140	1.160	2.210	1.070
21	.888	1.101	1.180	1.245	2.465	1.082
24	.985	1.140	1.277	1.305	1.420	1.122
27	1.038	1.152	1.226	1.260	1.116	1.100
30	1.096	1.194	1.231	1.265	1.063	1.152

TABLE XIX
N. A. C. A. 86
10° SWEEPFORWARD
NORMAL-FORCE COEFFICIENTS

α	C_N'					C_N total wing
	Sec. A	Sec. B	Sec. C	Sec. D	Sec. E	
Degrees						
−9	−0.435	−0.590	−0.505	−0.382	−0.622	−0.455
−6	−.143	−.292	−.311	−.227	−.343	−.108
−3	.136	−.045	−.065	−.058	−.117	.052
0	.447	.266	.201	.136	.129	.350
3	.700	.500	.404	.304	.357	.575
6	.920	.700	.577	.460	.630	.775
9	1.104	.915	.804	.655	.915	.970
12	1.265	1.110	.946	.792	1.200	1.148
15	1.070	1.063	1.030	.987	1.470	1.060
18	.843	1.038	1.120	1.090	1.750	.985
21	.862	.971	1.120	1.102	1.590	.996
24	.940	1.038	1.129	1.129	.960	1.103
27	.985	1.070	1.110	1.110	.856	1.016
30	1.062	1.130	1.162	1.150	.850	1.068

TABLE XX

N. A. C. A. 86

10° SWEEPBACK

NORMAL-FORCE COEFFICIENTS

α	C_N'					C_N total wing
	Sec. A	Sec. B	Sec. C	Sec. D	Sec. E	
Degrees						
−9	−0.446	−0.500	−0.558	−0.383	−0.091	−0.427
−6	−.175	−.266	−.305	−.214	−.045	−.207
−3	.110	−.019	−.065	−.053	−.019	.045
0	.376	.266	.188	.123	.026	.290
3	.648	.500	.396	.253	.053	.511
6	.875	.713	.590	.389	.097	.719
9	1.058	.901	.735	.552	.182	.893
12	1.207	1.102	.915	.655	.272	1.060
15	1.154	.796	.765	.700	.363	.960
18	.883	.720	.746	.720	.383	.805
21	.856	.752	.752	.740	.402	.806
24	.883	.817	.830	.799	.422	.855
27	.948	.900	.920	.862	.474	.935
30	1.000	.960	.980	.915	.486	.995

TABLE XXI

N. A. C. A. 86

20° SWEEPBACK

NORMAL-FORCE COEFFICIENTS

α	C_N'					C_N total wing
	Sec. A	Sec. B	Sec. C	Sec. D	Sec. E	
Degrees						
−9	−0.507	−0.456	−0.474	−0.337	−0.065	−0.455
−6	−.201	−.311	−.344	−.240	−.045	−.226
−3	.071	−.052	−.104	−.035	−.019	.007
0	.330	.214	.143	.104	.032	.252
3	.603	.460	.370	.253	.065	.486
6	.805	.655	.545	.383	.091	.674
9	.997	.862	.745	.532	.110	.858
12	1.160	1.039	.836	.596	.149	.990
15	1.278	.935	.655	.584	.279	1.028
18	1.039	.740	.603	.552	.253	.865
21	.970	.740	.616	.565	.253	.840
24	.985	.772	.675	.610	.279	.853
27	1.026	.843	.740	.675	.305	.914
30	1.082	.895	.824	.752	.344	.980